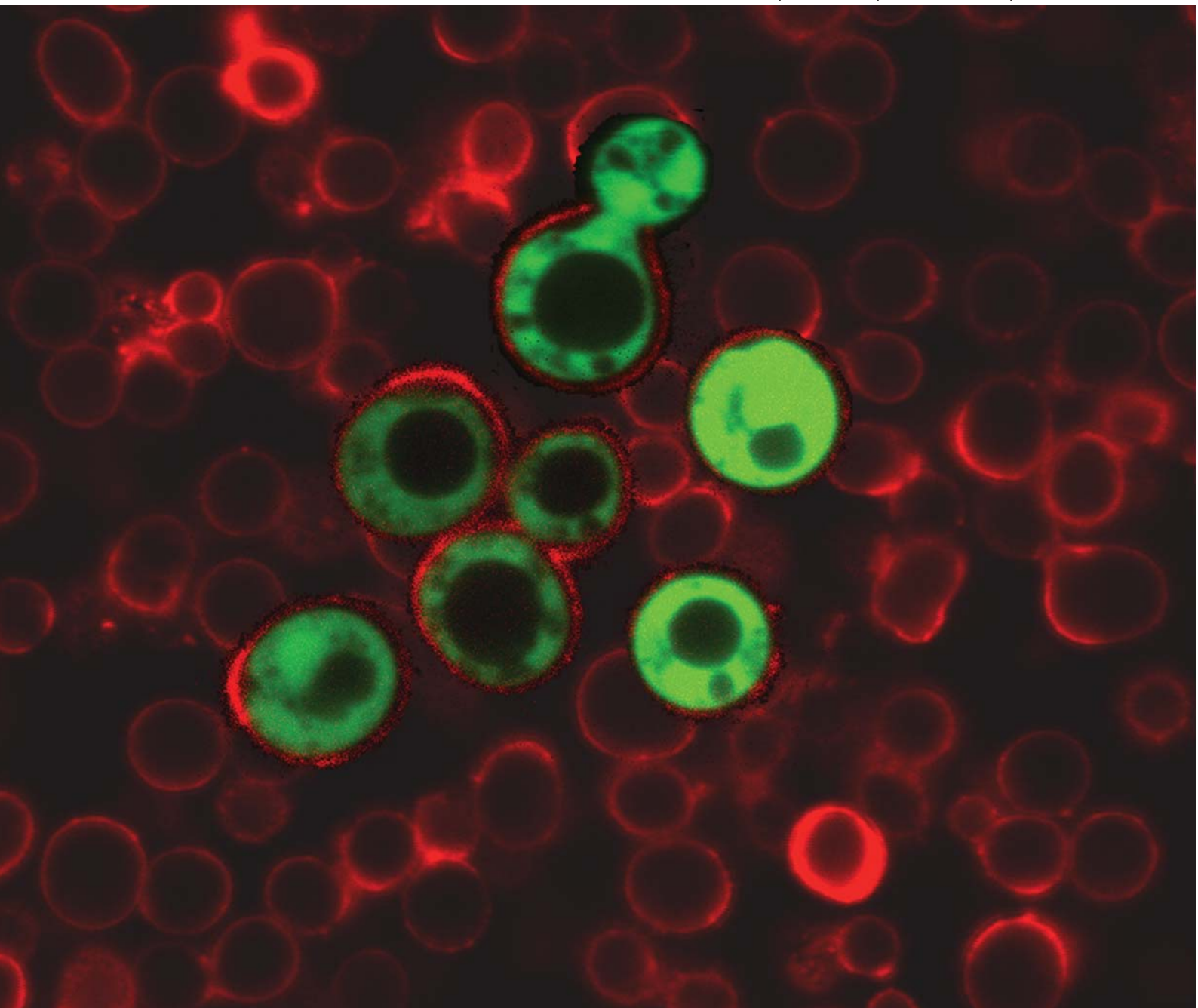


Soft Matter

www.rsc.org/softmatter

Volume 7 | Number 6 | 21 March 2011 | Pages 2165–3024



ISSN 1744-683X

RSC Publishing

PAPER

Vladimir V. Tsukruk *et al.*
Hydrogen-bonded LbL shells for living cell surface engineering

Cite this: *Soft Matter*, 2011, **7**, 2364

www.rsc.org/softmatter

PAPER

Hydrogen-bonded LbL shells for living cell surface engineering

Veronika Kozlovskaya,^a Svetlana Harbaugh,^b Irina Drachuk,^a Olga Shchepelina,^a Nancy Kelley-Loughnane,^b Morley Stone^b and Vladimir V. Tsukruk^{*a}

Received 28th September 2010, Accepted 17th November 2010

DOI: 10.1039/c0sm01070g

We report on the design of cytocompatible synthetic shells from highly permeable, hydrogen-bonded multilayers for cell surface engineering with preservation of long-term cell functioning. In contrast to traditional polyelectrolyte layer-by-layer (LbL) systems, shells suggested here are based on hydrogen bonding allowing gentle cell encapsulation using non-toxic, non-ionic and biocompatible components such as poly(*N*-vinylpyrrolidone) (PVPON) and tannic acid (TA) which were earlier exploited on abiotic surfaces but never assembled on cell surfaces. Here, we demonstrate that these LbL shells with higher diffusion facilitate outstanding cell survivability reaching 79% in contrast to only 20% viability level achieved with ionically paired coatings. We suggest that the drastic increase in cell viability and preservation of cell functioning after coating with synthetic shell stems from the minimal exposure of the cells to toxic polycations and high shell permeability.

Introduction

Surface engineering of living cells with natural or synthetic compounds is considered an efficient way to regulate cell functioning and protect them from hostile environment.^{1–3} Cell surface modification can enhance stability of biological species, mediate intercellular communication and render them insensitive to environmental changes.^{4–6} Current cell modification strategies are mostly based on covalent conjugation to amine groups of surface proteins, incorporation of amphiphilic molecules, such as PEG-phospholipids into the lipid bilayer membrane, and cell decoration with/inclusion into biodegradable gel microparticles.^{7–11} However, for these strategies, modification agents have been reported to disappear either by uptake into the cell interior or by dissociation from the cell surface.^{12,13} Furthermore, the presence of the thick synthetic materials can adversely interfere with cell functioning by hindering diffusion of nutrients.¹⁴ The ability to tailor permeability is particularly important for encapsulation of living cells with preservation of their functionalities as cell viability critically depends on the diffusion of nutrients through the synthetic shells. Thus, various strategies have been proposed with layer-by-layer (LbL) assembly considered as a valuable method for cell surface engineering.^{15–18}

Indeed, assembly of cationic and anionic polymers has been demonstrated as a versatile approach for formation of nanoscale membranes,^{19,20} nanocomposite membranes,^{21–23} shells,^{24–26} and nanoporous barriers.^{27–29} The advantages of this approach for

cell surface modification include conformal coating of geometrically challenged templates, a precise control of the membrane nanoscale thickness, and wide tunability of membrane functionalities and properties.^{30–37} The ability to tailor permeability properties by the LbL approach is of particular importance for encapsulation of living cells as cell viability critically depends on the diffusion of nutrients through the artificial polymer membrane. The poly(allylamine hydrochloride)/poly(styrene sulfonate) (PAH/PSS) coating is the mostly explored polyelectrolyte pair used to encapsulate cells.^{38–41}

Despite successful examples of the LbL-based cell encapsulation, cytotoxicity of the polycations posed severe limitations on this approach for cell surface engineering.^{42,43} As suggested, overall toxicity of the PAH/PSS LbL shells originates from the positive charge of cationic polyelectrolytes which cause cell membrane pores formation followed by cell damage and death.^{44,45} For instance, four bilayers of poly(L-lysine)/PSS, poly(ethyleneimine)/PSS, and PAH/PSS resulted in significant decreases in viability and death of mammalian cells.⁴⁶ A (PLL/alginate)₂ multilayers demonstrated extreme toxicity for human pancreatic islets resulting in their instant death.⁴⁷ The reduction in the toxicity can be achieved by decreasing the polycation charge density through grafting of PEG chains to generate PLL-*g*-PEG cytocompatible copolymers.^{47,48} However, most of the existing approaches do not provide a reliable method for *long-time functioning of individual cells* due to limited diffusion of nutrition *via* thick shells or interference from cationic components.

Therefore, to design cytocompatible synthetic shells capable of long-term support of cell functioning, here we introduce novel, highly permeable, hydrogen-bonded LbL nanoscale shells for cell surface engineering. In contrast to traditional ionically paired

^aSchool of Materials Science and Engineering, Georgia Institute of Technology, Atlanta, GA, 30332, USA. E-mail: vladimir@mse.gatech.edu

^bAir Force Research Laboratory, Directorate of Human Effectiveness, Wright-Patterson AFB, Dayton, OH, 45433, USA

polyelectrolyte LbL multilayers widely employed to date, LbL shells suggested here are based on hydrogen bonding allowing gentle cell encapsulation using non-toxic, non-ionic and biocompatible components such as poly(*N*-vinylpyrrolidone) (PVPON) and tannic acid (TA) which were exploited on abiotic surfaces but never assembled on cell surfaces.⁴⁹ TA was selected because of its ability of assembling with PVPON into hydrogen-bonded multilayers of high pH stability.⁴⁹ Also, as known, tannic acid possesses antioxidant and antibacterial properties and can inhibit radical-induced oxidation thus providing for enhanced cell viability.^{50–52} In this study, we demonstrate that these LbL shells with higher diffusion facilitate outstanding long-term (up to six days) cell survivability reaching 79% in contrast to only about 20% viability level with conventional PSS/PAH coatings.

Saccharomyces cerevisiae yeast cells were selected as a model of eukaryotic cells with completely sequenced genome which can be used in biosensors.^{53,54} *S. cerevisiae* with incorporated green fluorescent protein reporters (yEGFP) has been used for enzyme and protein analysis.^{55–57} The yEGFP-expressing yeast strains can offer an advantageous platform for cell-based sensors due to the rising fluorescence from yEGFP in response to a certain inducer and due to the cell ability to sporulate. During sporulation process, reproductive structures (*i.e.*, spores) are created. The spores can adapt and survive under unfavorable conditions for a long time which is highly desirable for cell-based biosensors.⁵⁸

Results and discussion

Morphology of LbL shells

The YPH501 cells were sequentially coated with (TA/PVPON)_{*n*} LbL shells through hydrogen-bonding between hydroxyl groups of TA and carbonyl groups of PVPON under deposition conditions which preserved cell integrity and functioning^{59–62} (see Experimental). Fig. 1 illustrates the LbL assembly of hydrogen-bonded shells around living cells. To ensure the adhesion of the following multilayers, cell surfaces were primed with

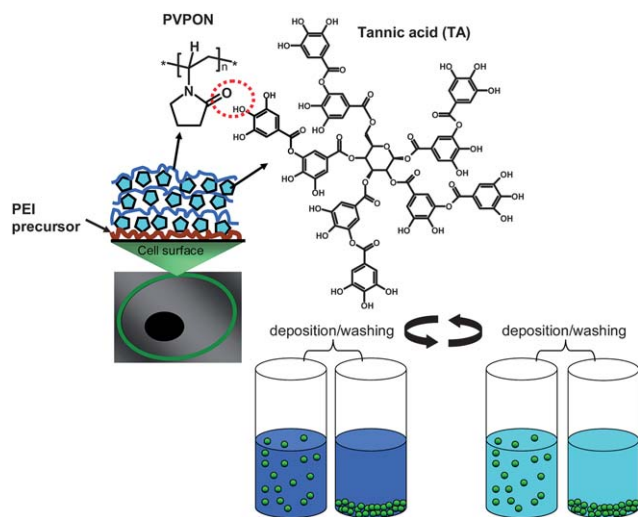


Fig. 1 Schematic illustrating formation of hydrogen-bonded TA/PVPON shell layer-by-layer on yeast cell surfaces and LbL assembly of hydrogen-bonded layers.

a poly(ethyleneimine) (PEI) monolayer which was possible due to negatively charged cell surface (-30 ± 3 mV). The adsorption of PEI was performed at pH = 7 (0.1 M) to reduce the positive charge on the precursor backbone and reduce the amount of deposited PEI which can affect cell functioning.⁶³

The successful formation of the shells around the cells was initially confirmed by confocal microscopy. Fig. 2a–d demonstrate homogeneous fluorescence from Alexa Fluor 532-fluorescently tagged PVPON confirming formation of the polymer membrane. Fig. 2a demonstrates large scale confocal image of encapsulated yeast cells with fluorescently labeled PVPON-co-Alexa Fluor 532. Fig. 2b shows the same area in transmitted mode. By overlapping images from both fluorescent and transmitted modes (Fig. 2c), one can confirm that *all the cells* visible in the selected area have been coated. Fig. 2d presents high magnification confocal image of the wrapped cell showing uniform polymer coating around the cells. TEM analysis further confirms the CLSM data and demonstrates the integrity of the cell membrane upon adsorption of the PEI(TA/PVPON)₆ hydrogen-bonded shell (Fig. 2e and f). To study surface morphology of the coating, we prepared model hollow PEI(TA/PVPON)₆ shells using silica template particles. After removal of core particles and deposition on a solid substrate, AFM has been employed to reveal fine details of shell morphology. AFM images show grainy surface morphology of the hollow shells dried on a silicon wafer with domain dimensions about 50 nm and high concentration of small nanopores (Fig. 3).

The thickness of the shells increased linearly with the number of bilayers from 13 to 22 nm indicating a regular growth mode (Fig. 4). The average TA/PVPON bilayer thickness from AFM cross-sections was 4.0 ± 0.2 nm which is as twice as high compared to that of the LbL film adsorbed from low ionic strength solutions (1.7 ± 0.2 nm). This difference for the film formed under higher salt conditions is characteristic for the hydrogen-bonded LbL assembly and results from charge screening and decreased polymer solubility. Moreover, the surface microroughness of the LbL films increased significantly as a function of bilayer number from 2.2 to 3.1 nm (Fig. 4). Such an increase in surface microroughness is consistent with steady development of domain morphology which is caused by weak aggregation of hydrogen bonded components.

To assure the neutrality of the encapsulated yeast cells, we performed ζ -potential measurements as a function of the number of deposited layers for both haploid and diploid cells (Fig. 5). As confirmed by these measurements, the initial negative charge of the cell membrane was partially neutralized after deposition of the precursor PEI layer, and was completely neutralized after 3–4 layer deposition on cell surface, making LbL encapsulated cells completely neutral.

Encapsulated cell viability

The viability of cells with different LbL shells was assessed with the resazurin assay.⁶⁴ As schematically shown in Fig. 6a, bio-reduction of resazurin by reducing enzyme cofactors in viable cells results in the conversion of the resazurin oxidized blue form to its pink fluorescent intermediate, resorufin.⁶⁵ The absence of such cofactors in dead cells leads to no conversion and no fluorescence can be detected.⁶⁶ The cells coated with the

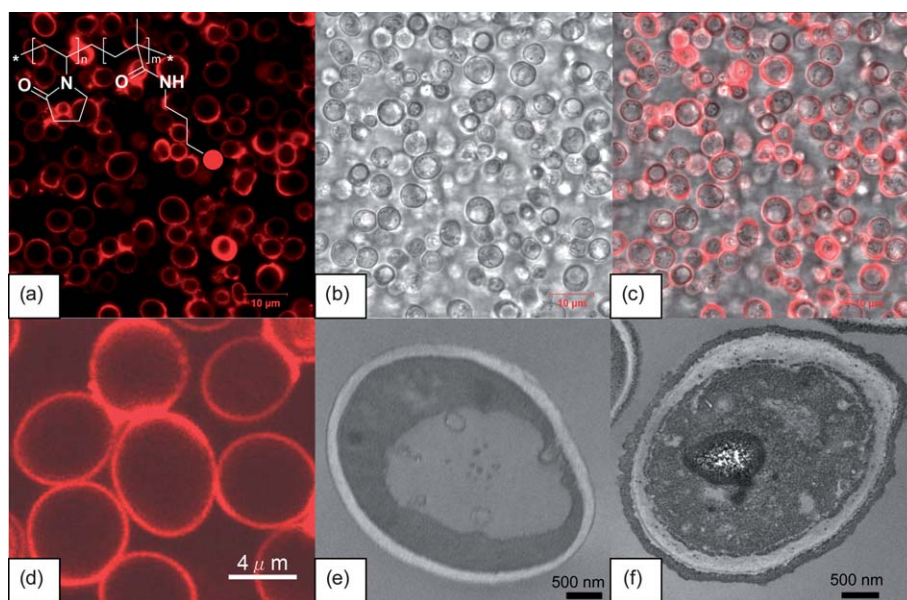


Fig. 2 Confocal images of YPH501 *S. cerevisiae* yeast cells encapsulated with layers of PEI(TA/PVPON)₄ before yEGFP expression (a–c). Image (a) shows encapsulated yeast cells with fluorescently labeled PVPON-co-Alexa Fluor 532 (Ex/Em = 543/560) as the top layer. Image (b) shows yeast cells in transmitted mode, (c) is the stack image of (a) and (b) together, and (d) is higher magnification image of encapsulated cells. TEM images of freeze-dried bare (e) and PEI(TA/PVPON)₆-coated (f) YPH501 yeast cells.

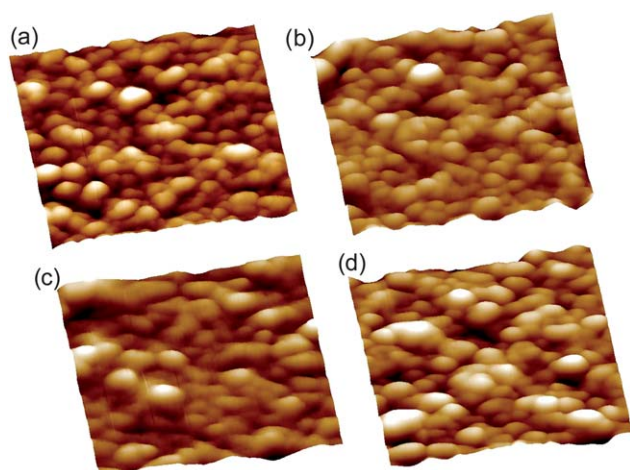


Fig. 3 3D topographical AFM images of PEI(TA/PVPON)_n hollow shells dried on a silicon wafer with $n = 3$ (a), $n = 4$ (b), $n = 5$ (c), and $n = 6$ bilayers (d). Scale is 500 nm × 500 nm × 50 nm.

(TA/PVPON)_n layers showed high viability up to the thickest shells studied here (Fig. 6).

To test the hypothesis that the presence of ionic components is responsible for LbL shell cytotoxicity and shell permeability is critical for long-term survival, we conducted comparative studies of hydrogen-bonded and ionic LbL shells as well as measured diffusion of small and large molecules across the LbL shells.

Unlike the PAH/PSS, hydrogen-bonded shells exert much lower, 5%, cytotoxicity with each following bilayer assembled. We attribute the initial decrease in cell viability in the case of PEI(TA/PVPON)_n shell to the PEI pre-layer. Notably, assembly of 3- and 4-bilayer PEI(TA/PVPON) LbL shells maintained high viability up to 79% in contrast to polyelectrolyte (PAH/PSS)

shells (Fig. 6). Indeed, in contrast to current shells, 3 and 4 bilayers of ionic (PAH/PSS) shell caused up to 88% of cell death which is consistent with the PAH/PSS cytotoxicity vastly reported in literature (Fig. 6).¹

To estimate the permeability of low molecular weight molecule, fluorescein isothiocyanate (FITC), through PEI(TA/PVPON) shells, we utilized spherical silica templates. After the silica cores were removed and the hollow polymer shells were obtained, we used FRAP experiments to model the permeability of nutrients through the shells (see Experimental).⁶⁷ As seen, the permeability through the hydrogen-bonded shell is dramatically higher for comparable number of PAH/PSS bilayers with diffusion coefficient reaching $D = 8 \times 10^{-12} \text{ cm}^2 \text{ s}^{-1}$ which is almost five times higher than that known for traditional polyelectrolyte LbL shells (Fig. 7).⁶⁸ The data points for permeation through the PAH/PSS shells were taken from literature and plotted for comparison.⁶⁸ The diffusion coefficient decrease with the increasing number of bilayers implies the diffusion limiting permeation.⁶⁹ The observed difference for diffusion coefficients between PAH/PSS and TA/PVPON shells can be attributed to loose, grainy morphology of the TA/PVPON LbL multilayers characteristic for hydrogen-bonded systems.⁷⁰ These results support our suggestion on the highly permeable structure of hydrogen-bond shells exploited here which is critical for the transport of nutrients towards coated cells.

Moreover, our results on polysaccharides diffusion across LbL shells suggested the threshold of the shell permeability between 20 and 40 kDa under the experimental conditions.⁶² Considering reported size of the FITC-dextrans of 1.5 and 2.2 nm, respectively, the mesh size of the (TA/PVPON)₄ network can be estimated to be within this range under these assembling conditions.⁷¹ Indeed, the AFM analysis of the shells confirmed grainy surface morphology and the microroughness of 3 nm

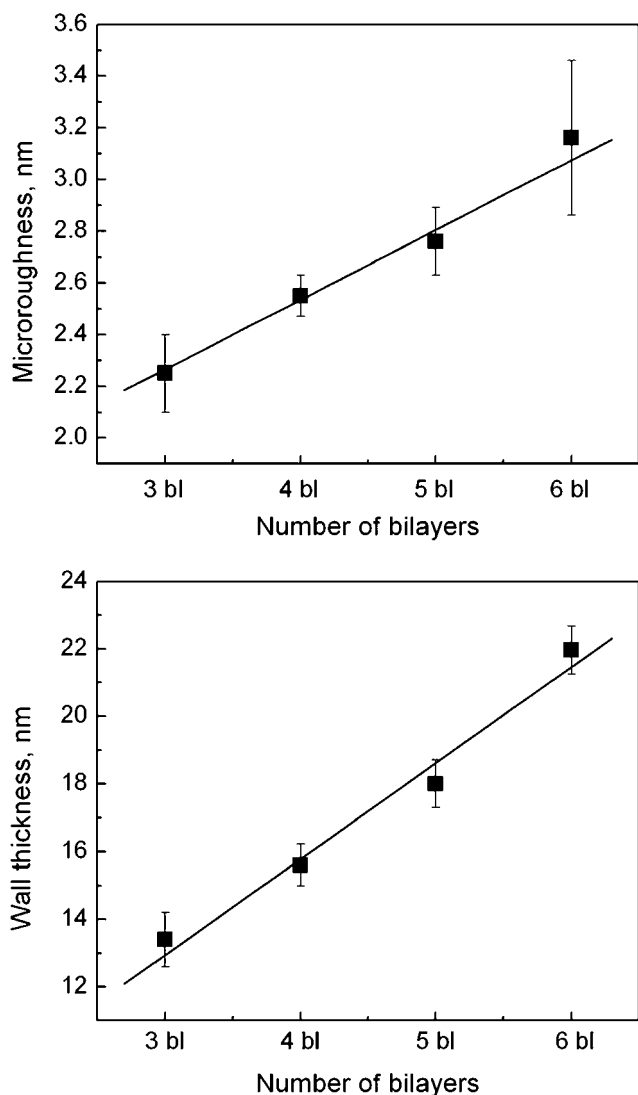


Fig. 4 Wall thickness of PEI(TA/PVPON)_n capsules (bottom) and root mean square roughness (top) as measured by AFM in dry state with respect to the number of bilayers.

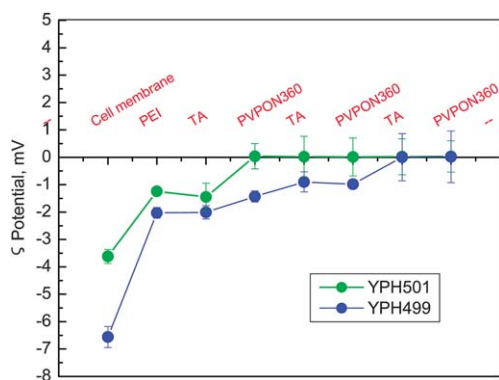


Fig. 5 ζ -Potential of encapsulated yeast cells YPH501 and YPH499 at pH 6. YPH501 and YPH499 cells were encapsulated with PEI(TA/PVPON)₃ at pH 6.

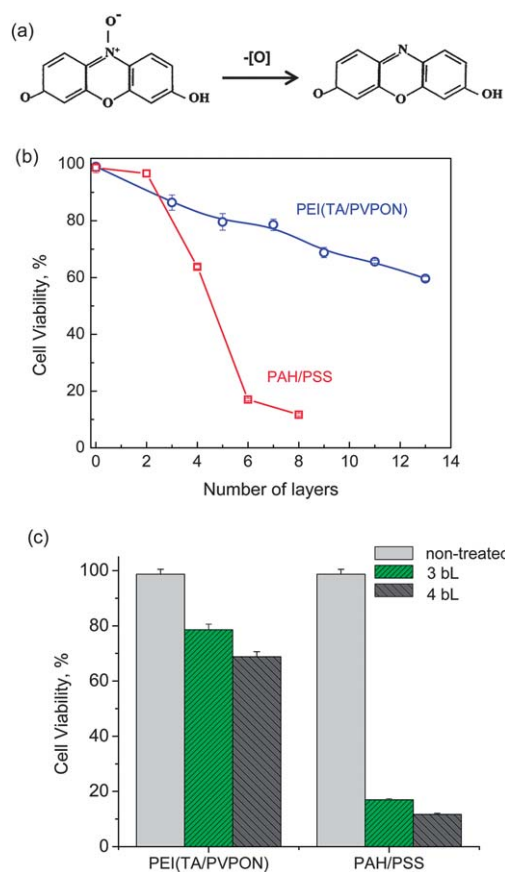


Fig. 6 (a) A schematic showing bioreduction of resazurin by viable cells from its oxidized blue form (left) to its pink colored, fluorescent intermediate resorufin (right). (b) Comparison of cell viability (%) for (PAH/PSS) and (TA/PVPON) coatings tested with resazurin assay. (c) Cell viability (%) of non-treated YPH501 yeast cells (control) in comparison to PEI(TA/PVPON)_{3,(4)} and (PAH/PSS)_{3,(4)}-coated cells.

(within $1 \times 1 \mu\text{m}^2$), well exceeding microroughness of 0.5 nm for uniform, smooth PSS/PAH coatings without any pores presented⁷² (Fig. 3 and 4).

Cell surface engineering with hydrogen-bonded shells supports important functional ability of the yeast cells to produce a reporter protein (yEGFP) in response to an inducer molecule

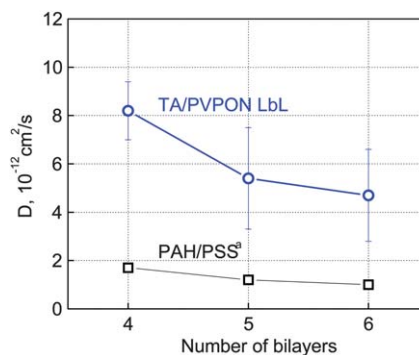


Fig. 7 FITC diffusion coefficient as a function of the number of (TA/PVPON) layers. Diffusion data points for PAH/PSS shells are presented for comparison.⁶⁸

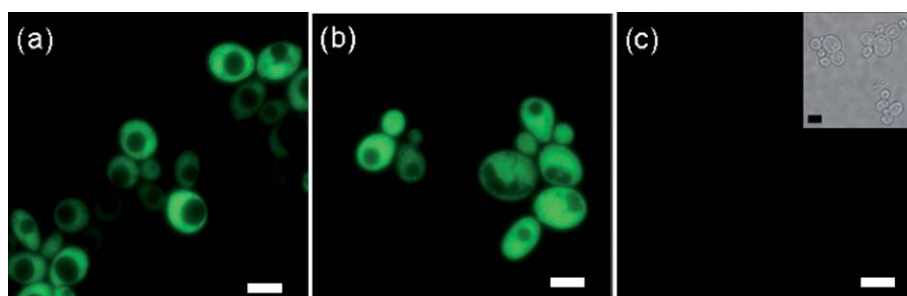


Fig. 8 Optical fluorescence images of non-treated (a), PEI(TA/PVPON)₃- (b) and (PAH/PSS)₃-coated cells (c) after expression of yEGFP was induced. Inset shows a transmittance optical image of the same area for (c). Scale bars are 5 μm.

(Fig. 8). Optical fluorescence microscopy of control and PEI(TA/PVPON)₃- or (PAH/PSS)₃-coated cells shows that hydrogen-bonded shell does not interfere with the yEGFP expression and

fluorescence emission from the cells can be easily observed (Fig. 8a and b). By contrast, no fluorescence from (PAH/PSS)₃ coated yeast cells can be detected that indicates suppression of the yEGFP-reporter function of cells coated with PAH/PSS multilayers, as a result, the fluorescence image appears completely black (Fig. 8c). The same surface area observed under transmission mode revealed the presence of the (PAH/PSS)₃-coated cells (Fig. 8c, inset).

Moreover, continuous monitoring of the yEGFP fluorescence from coated yeast cells after induction of the reporter protein expression showed that gradually increased fluorescence can be detected from the cells coated with 3, 4, 5, and 6 bilayers of TA/PVPON shell (Fig. 9a). For comparison, the fluorescence intensity from 4-bilayer (TA/PVPON) coated cells was almost 13 times higher than that from (PAH/PSS)₄-coated cells indicating dramatic difference in activities of these counterparts (Fig. 9b).

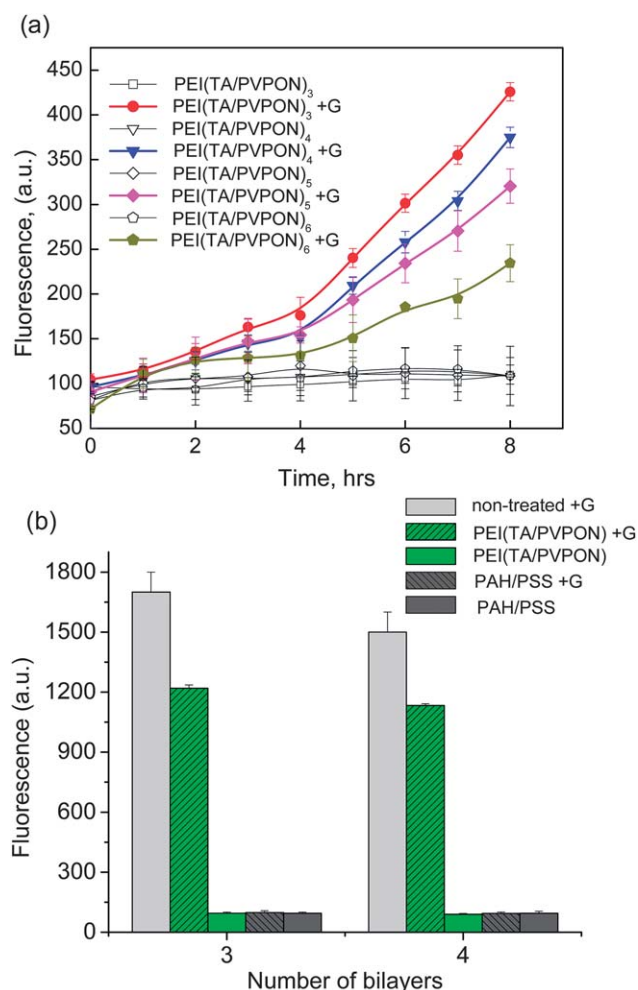


Fig. 9 (a) Expression of fluorescent yEGFP by yeast YPH501 cells encapsulated in PEI(TA/PVPON) with varied thickness of hydrogen-bonded membrane. The galactose-induced samples are denoted as PEI(TA/PVPON)_n+G, while the control samples without galactose are denoted as PEI(TA/PVPON)_n, with *n* denoting the number of bilayers. (b) Comparison of the yEGFP fluorescence intensity from the non-treated (control) cells and PEI(TA/PVPON)- or PAH/PSS-coated cells after 16 hours (b).

Encapsulated cell growth

Preserved cell function and viability are indicated by their ability to bud after cellular surfaces were modified with the LbL shells. Fig. 10a demonstrates the characteristic S-shaped cell growth of control cells and PEI(TA/PVPON)-coated cells. During the initial lag phase the rate of growth, or cell division, is slow in all cases. Red fluorescence in confocal images of the PEI(TA/PVPON)₃-coated cells taken in the lag phase witnesses a homogenous polymer coating around cells (Fig. 10b). Moreover, the green fluorescence from the yEGFP-reporter produced by the yeast cells confirms that this functional capacity of the cells was not adversely influenced by the presence of shell. This stage is followed by the exponential growth mode when cell division accelerates and a unicellular organism duplicates, *i.e.*, one cell produces two in a given period of time (see divided cells as indicated by arrows in Fig. 10c). During this phase very rapid multiplying of yeast cells is observed by reading absorbance (optical density) at 600 nm. The exponential phase then proceeds to a stationary phase when there is no discernible change in cell concentration.

While original yeast cells go into the exponential phase after eight hours duplicating every four hours (data not shown), there is a delay of the exponential phase for the TA/PVPON-coated cells which is dependent on the thickness of the polymer coating (Fig. 10a, circles and squares, respectively). Confocal imaging of the PEI(TA/PVPON)₃-coated cells before the stationary phase revealed that during exponential growth coated cells are able to

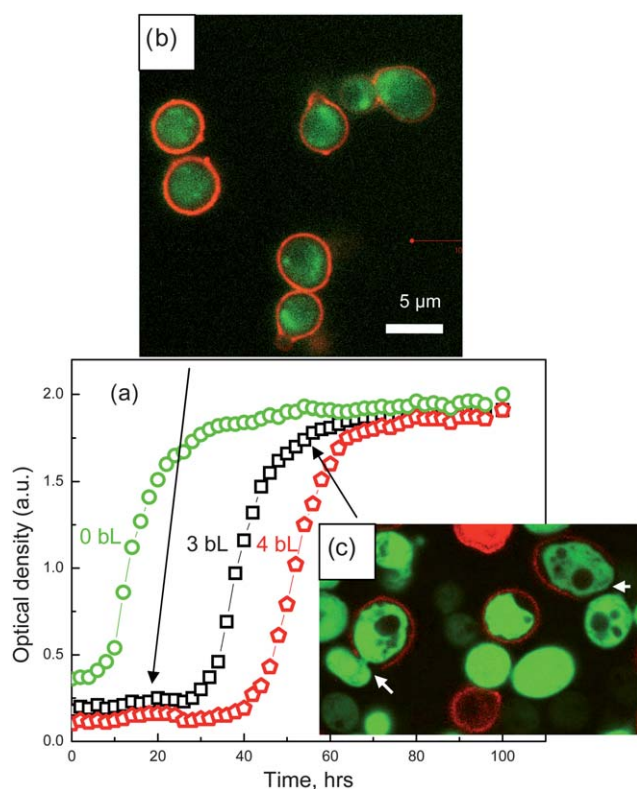


Fig. 10 Growth of PEI(TA/PVPON)_{0,(3),(4)}-coated YPH501 cells after yEGFP expression was induced (a). Confocal microscopy images of PEI(TA/PVPON)₃-coated cells after 10 hours (b) and 46 hours (c) of the yEGFP expression.

break the polymer shell suggesting that the coating delays but does not suppress cell division (Fig. 10c). This is similar to polycation/polyanion coatings and is due to comparable rigidity of the TA/PVPON coatings which exhibit Young's modulus of 1.8 ± 0.4 GPa in dry state (buckling test⁷³), similar to that of the PAH/PSS system (1–4 GPa).^{19,74}

Conclusions

Herein, we report on a new approach for cell surface modification through LbL assembly of nanoscale hydrogen-bonded shells with inclusion of tannic acid as a critical component which allows for maintaining high viability of the wrapped cells over a long time (up to 6 days in current studies). The important cell function to express yEGFP reporter has been preserved in the (TA/PVPON)₆-coated yeast cells with viability reaching 79% while it was almost completely suppressed with (PAH/PSS)_n shells of only 6 nm thickness. This high cytocompatibility originates not only from the minimal exposure of the cells to toxic polycations but also from highly permeable LbL shells favoring an easy access of nutrients and inducer molecules to cell interior unachievable with previously reported polyelectrolyte LbL shells. Moreover, the hydrogen-bonded LbL shell design suggested here opens a new path to create pH sensitive encapsulation with mediated permeability and elasticity, already observed for some TA-based LbL structures,^{49,75} which is a subject of our current studies. Such non-cytotoxic and potentially responsive hydrogen-bonded LbL

assembly of non-ionic components suggests a promising tool for living cell surface engineering for biomedical and biosensing applications.

Experimental

Materials

Tannic acid (TA) ($M_w = 1700$ Da), branched poly(ethyleneimine) (PEI) ($M_w = 25\ 000$ Da), poly(*N*-vinylpyrrolidone) ($M_w = 360\ 000$ Da) (PVPON), mono- and dibasic sodium phosphate, *N*-vinylpyrrolidone (VPON), galactose, and glucose were purchased from Sigma-Aldrich. Silica particles with a diameter of 4.0 ± 0.2 μm as 10% dispersions in water, and monomer, *N*-(*tert*-butoxycarbonyl-amino-propyl)methacrylamide (*t*-BOC), were from Polysciences, Inc. Hydrofluoric acid (48–51%) was purchased from BDH Aristar. Alexa Fluor 532 carboxylic acid succinimidyl ester fluorescent dye was purchased from Invitrogen. Ultrapure (Nanopure system) filtered water with a resistivity of 18.2 MΩ cm was used for experiments. Initiator, 2,2'-azobis(2-methylpropanitrile) (AIBN), was purchased from Sigma-Aldrich and re-crystallized from methanol at around 30 °C before use.

The *S. cerevisiae*, YPH499 haploid and YPH501 diploid yeast strains expressing yEGFP (yeast enhanced green fluorescence protein) were used for this study. Cells were cultured in synthetic minimal medium (SMM) supplemented with appropriate dropout solution and sugar source, 2% glucose. Yeast cells were grown at 30 °C in a shaker incubator (New Brunswick Scientific) with 225 rpm to bring them to an early exponential phase.

Synthesis of fluorescently tagged poly(*N*-vinylpyrrolidone) (Alexa Fluor 532–PVPON)

PVPON-*co*-NH₂ copolymer was synthesized using gradual feeding copolymerization of VPON and *t*-BOC as described previously.⁷⁶ The reaction yield was 56%. *t*-BOC protecting groups were hydrolyzed by treating the copolymer with 1 M HCl in methanol for 100 hours.⁷⁶ Solutions of the deprotected copolymers were dialyzed against Milli-Q water using a Slide-A-Lyzer Dialysis Cassette (Thermo Scientific) with a molecular weight cutoff of 10 kDa and lyophilized (FreeZone 4.5 Liter Benchtop Freeze Dry System). Composition of the resultant amino-containing copolymer prior and/or after hydrolysis of BOC-protective groups was determined using the NMR technique (Bruker DSX 400). The copolymer contained 4.2% of amine groups. The molecular weight of PVPON-*co*-NH₂ was determined using GPC (Waters, 717 plus). A calibration curve based on linear polystyrene standards was used in conjunction with a differential refractive index detector (Waters, 2414). The molecular weight of the resultant amino-containing PVPON copolymer was determined to be 20 kDa ($M_n = 17$ kDa, PDI = 1.2). Amino-containing copolymer PVPON-*co*-NH₂ was reacted with Alexa Fluor 532 carboxylic acid succinimidyl ester fluorescent dye in methanol overnight in the dark to produce Alexa Fluor 532–PVPON fluorescently tagged polymer.⁷⁷ The Alexa Fluor 532–PVPON was exhaustively dialyzed against deionized water for 5 days. The dialysis was completed after no fluorescence was detected in the dialysis water. The dialyzed polymer

solution was lyophilized, and solutions of Alexa Fluor 532–PVPON were prepared.

Encapsulation of cells with hydrogen-bonded TA/PVPON shells

The LbL assembly was employed for encapsulation of individual yeast cells with hydrogen-bonded multilayers of TA/PVPON.^{49,62} Before deposition of PEI(TA/PVPON)_{*n*} multilayer membrane, where *n* denotes the number of deposited bilayers, yeast cells were harvested in 15 mL centrifuge tubes by centrifugation at 2000 rpm for 4 minutes and washed three times in phosphate buffer (0.01 M in 0.1 M NaCl, pH = 6). First, a precursor, PEI, was allowed to adsorb onto yeast cell membrane from 0.5 mg mL⁻¹ aqueous solution (0.1 M NaCl, pH = 7) for 15 min followed by the LbL deposition of hydrogen-bonded TA/PVPON layers from solutions of the same concentrations dissolved in 0.01 M phosphate buffer and 0.1 M NaCl at pH = 6. During LbL deposition, cells were re-dispersed in the appropriate solution by gentle shaking (at 225 rpm) for 15 minutes. After deposition of each layer, cells were collected in a pellet by centrifugation and washed three times with phosphate buffer.

To visualize the polyelectrolyte membrane in CLSM, Alexa Fluor 532–PVPON was used during the deposition of the outermost (TA/PVPON) bilayer. All solutions were filter-sterilized with polystyrene nonpyrogenic membrane systems (0.22 μm pore size) (Corning filter system) before applying to the cells. When hollow shells of PEI(TA/PVPON)_{*n*} were needed for diffusion experiments, the hydrogen-bonded multilayers were assembled onto silica particles in the same manner described above.⁶²

Confocal laser scanning microscopy (CLSM)

Confocal images of encapsulated and non-encapsulated yeast cells were obtained with an LSM 510 NLO META inverted confocal microscope equipped with 63 × 1.4 oil immersion objective lens (Zeiss, Germany). Before imaging, cells were washed three times in deionized water to reduce background auto-fluorescence from the SMM medium. Coated or uncoated yeast cells were seeded in Lab-Tek chamber glasses (Electron Microscopy Sciences) for half an hour before imaging. The 488 nm excitation from the Argon ion laser and 514 nm emission wavelengths were used for yEGFP visualization, whereas 543 nm excitation (He–Ne laser) and 565 nm emission were used to visualize fluorescently labeled polymer shells surrounding yeast cells.

ζ-Potential measurements

Independent measurements of ζ-potentials on bare yeast cells of two strains YPH501 and YPH499, and encapsulated yeast cells after deposition of each layer were performed on Zetasizer Nano-ZS equipment (Malvern). Yeast cells were collected at mid-log phase (OD = 0.6–0.8), washed three times in the solution of 0.01 M phosphate buffer and 0.1 M NaCl at pH 6.0 before performing deposition of subsequent layers of PEI, TA and PVPON (*M_w* = 360 kDa) followed by alteration of TA and PVPON layers. After deposition and washing, 100 μL of encapsulated cells were combined with 900 μL of deionized Nanopure water to obtain 1 mL of solution to perform ζ-potential measurements.

Each value was acquired by averaging three independent measurements of 40 sub-runs each.

Cell growth and expression of yEGFP

Encapsulated cells were incubated in 2% raffinose and 2% galactose in SMM yeast media at 30 °C to induce the yEGFP production. Optical density at 600 nm (OD600) and fluorescence were measured at indicated time points. The coated cells were cultured in the presence of galactose instead of glucose to induce expression of yEGFP.

Transmission Electron microscopy (TEM)

TEM images of encapsulated and non-encapsulated yeast cells were captured with a Hitachi H-7600 Transmission Electron microscope. All samples were fixed with 2% of paraformaldehyde and stained with 1% osmium tetroxide in 0.1 M PBS buffer. Following staining, the cells were dehydrated using a graded series of ethanol (50%, 70%, 80%, 90%, and 100%). Embedding process involved re-suspending the dehydrated cells in 1 : 1 ratio of LR White resin to 100% of ethanol.

Atomic Force microscopy (AFM)

Surface topography of the hollow PEI(TA/PVPON)₄ and PEI(TA/PVPON)₆ capsules was examined using AFM. The AFM images were collected using a Dimension-3000 (Digital Instruments) microscope in the “light” tapping mode according to the well established procedure.⁷⁸ A drop of capsule suspension was placed onto a pre-cleaned silicon wafer and dried in air prior to imaging. For film thickness measurements the capsule single wall thickness was determined as half of the height of the collapsed flat regions on dried capsules using bearing analysis from NanoScope software to generate height histograms.^{79,80}

Fluorescence recovery after photobleaching (FRAP)

Experiments on permeability were performed using CLSM.⁸¹ Briefly, photobleaching of FITC fluorescent molecules inside the capsule was performed. Hollow capsules of hydrogen-bonded TA/PVPON with 4, 5 and 6 bilayers were prepared as described elsewhere.⁶² 100 μL of hollow capsules solution was combined with 200 μL of 1 mg mL⁻¹ FITC solution (pH = 6) and allowed to settle down in a Lab-Tek chamber glass cell for three hours. Laser beam (488 nm) was focused within a region of interest (ROI) inside a capsule, and pulsed at 100% intensity to photobleach the dye molecules. Each experiment started with 3 pre-bleached image scans followed by 25–35 bleach pulse exposures of 3 ms each within ROI. The bleaching time was adjusted to ensure complete photobleaching of FITC inside the capsule. The fluorescence recovery was monitored by capturing 30 scans of 3 ms exposure at 3% laser intensity. The recovery was considered complete when the intensity of the photobleached region stabilized. The quantitative analysis was performed using ImageJ software, and curve-fitting was conducted in Origin.

The recovery curve of the fluorescence intensity, *I*(*t*), as a function of time, *t*, was fit by:

$$I = I_0(1 - e^{-At}) \quad (1)$$

where $I_{\text{and}} I_0$ are the equilibrium and initial fluorescence intensities, respectively. The coefficient A is related to the diffusion coefficient, D , according to:

$$A = 3D/rh \quad (2)$$

for FITC diffusion through a spherical wall with radius r and thickness h .

In the solution, eqn (1) obeys Fick's law and can be written as:

$$dc/dt = -A(c - c_0) \quad (3)$$

where c and c_0 are the concentrations inside and outside the capsules, respectively, and $c \approx I$. A typical fit of the recovery curve was obtained using eqn (1) and the coefficient A was deduced from the fitting.^{82–84}

Cell viability tests

Live–dead cell staining. To evaluate the viability of individual cells encapsulated in the hydrogen-bonded TA/PVPON capsules, yeast cells were stained with Live–Dead Cell Staining Kit (Bio-Vision) according to the supplied protocol.

Resazurin assay. Control (non-treated) and encapsulated cells were re-suspended in 1 mL of media. 100 μL of resazurin (7-hydroxy-3*H*-phenoxazin-3-one 10-oxide) solution was added to cell cultures. The mixtures were incubated at 30 °C for 2 hours. Fluorescence was measured at $\lambda = 590 \text{ nm}$ ($\lambda_{\text{EX}} = 560 \text{ nm}$).

Acknowledgements

This work was supported by the Air Force Office of Scientific Research FA9550-08-1-0446 and FA9550-09-1-0162 grants. The authors acknowledge Richard Murdock and Dr Pamela Lloyd for TEM measurements and Dr Rajesh Naik for useful discussions.

References

- 1 Y. Teramura and H. Iwata, *Soft Matter*, 2010, **6**, 1081–1091.
- 2 P. R. Leduc, M. S. Wong, P. M. Ferreira, R. E. Groff, K. Haslinger, M. P. Koonce, W. Y. Lee, J. C. Love, J. A. McCammon, N. A. Monteiro-Riviere, V. M. Rotello, G. W. Rubloff, R. Westerwelt and M. Yoda, *Nat. Nanotechnol.*, 2007, **2**, 3–7.
- 3 E. C. Carnes, D. M. Lopez, N. P. Donegan, A. Cheung, H. Gresham, G. S. Timmins and C. J. Brinker, *Nat. Chem. Biol.*, 2010, **6**, 41–45.
- 4 M.-C. Raymond, R. J. Neufeld and D. Poncelet, *Artif. Cells, Blood Substitutes, Biotechnol.*, 2004, **32**, 275–291.
- 5 J. T. Wilson and E. L. Chaikof, *Adv. Drug Delivery Rev.*, 2008, **60**, 124–145.
- 6 F. Caruso, D. Trau, H. Moehwald and R. Renneberg, *Langmuir*, 2000, **16**, 1485–1488.
- 7 S. Zhang, M. A. Greenfield, A. Mata, L. C. Palmer, R. Bitton, J. R. Mantei, C. Aparicio, M. O. de la Cruz and S. I. Stupp, *Nat. Mater.*, 2010, **9**, 594–601.
- 8 S. Sakai, S. Ito and K. Kawakami, *Acta Biomater.*, 2010, **6**, 3132–3137.
- 9 Y. Teramura, Y. Kaneda, T. Totani and H. Iwata, *Biomaterials*, 2008, **29**, 1345–1355.
- 10 Y. Teramura and H. Iwata, *Bioconjugate Chem.*, 2008, **19**, 1389–1395.
- 11 V. H. Orozco, V. Kozlovskaya, E. Kharlampieva, B. L. López and V. V. Tsukruk, *Polymer*, 2010, **51**, 4127–4139.
- 12 D. Y. Lee, J. H. Nam and Y. Byun, *Biomaterials*, 2007, **28**, 1957–1966.

- 13 S. Cabric, J. Sanchez, T. Lundgren, A. Foss, M. Felldin, R. Kallen, K. Salmela, A. Tibell, G. Tufveson, R. Larsson, O. Korsgren and B. Nilsson, *Diabetes*, 2007, **56**, 2008–2015.
- 14 D. Rabuka, M. B. Forstner, J. T. Groves and C. R. Bertozzi, *J. Am. Chem. Soc.*, 2008, **130**, 5947–5953.
- 15 M. Chanana, A. Gliozzi, A. Diaspro, I. Chodnevskaja, S. Huewel, V. Moskalenko, K. Ulrichs, H.-J. Galla and S. Krol, *Nano Lett.*, 2005, **5**, 2605–2612.
- 16 S. Krol, S. del Guerra, M. Grupillo, A. Diaspro, A. Gliozzi and P. Marchetti, *Nano Lett.*, 2006, **6**, 1933–1939.
- 17 N. G. Veerabadran, P. L. Goli, S. Stewart-Clark, Y. M. Lvov and D. K. Mills, *Macromol. Biosci.*, 2007, **7**, 877–882.
- 18 O. Shchepelina, V. Kozlovskaya, S. Singamaneni, E. Kharlampieva and V. V. Tsukruk, *J. Mater. Chem.*, 2010, **20**, 6587–6603.
- 19 C. Jiang, S. Markutsya, Y. Pikus and V. V. Tsukruk, *Nat. Mater.*, 2004, **3**, 721–728.
- 20 C. Jiang and V. V. Tsukruk, *Adv. Mater.*, 2006, **18**, 829–840.
- 21 C. Jiang and V. V. Tsukruk, *Soft Matter*, 2005, **1**, 334–337.
- 22 C. Jiang, S. Markutsya, H. Shulha and V. V. Tsukruk, *Adv. Mater.*, 2005, **17**, 1669–1673.
- 23 D. Zimmitsky, C. Jiang, J. Xu, Z. Lin, L. Zhang and V. V. Tsukruk, *Langmuir*, 2007, **23**, 10176–10183.
- 24 F. Caruso, R. A. Caruso and H. Mohwald, *Science*, 1998, **282**, 1111–1114.
- 25 G. B. Sukhorukov, E. Donath, S. Davis, H. Lichtenfeld, F. Caruso, V. I. Popov and H. Mohwald, *Polym. Adv. Technol.*, 1998, **9**, 759–767.
- 26 E. Donath, G. B. Sukhorukov, F. Caruso, S. A. Davis and H. Mohwald, *Angew. Chem., Int. Ed.*, 1998, **37**, 2202–2205.
- 27 D. Zimmitsky, V. V. Shevchenko and V. V. Tsukruk, *Langmuir*, 2008, **24**, 5996–6006.
- 28 A. Fery, B. Schoeler, T. Cassagneau and F. Caruso, *Langmuir*, 2001, **17**, 3779–3783.
- 29 J. D. Mendelsohn, C. J. Barrett, V. V. Chan, A. J. Pal, A. M. Mayes and M. F. Rubner, *Langmuir*, 2000, **16**, 5017–5023.
- 30 P. T. Hammond, *Adv. Mater.*, 2004, **16**, 1271–1293.
- 31 J. F. Quinn, A. P. R. Johnston, G. K. Such, A. N. Zelikin and F. Caruso, *Chem. Soc. Rev.*, 2007, **36**, 707–718.
- 32 L. L. del Mercato, P. Rivera-Gil, A. Z. Abbasi, M. Ochs, C. Ganas, I. Zins, C. Soennichsen and W. J. Parak, *Nanoscale*, 2010, **2**, 458–467.
- 33 A. S. Hoffman, *Adv. Drug Delivery Rev.*, 2002, **43**, 3–12.
- 34 A. N. Zelikin, Q. Li and F. Caruso, *Chem. Mater.*, 2008, **20**, 2655–2661.
- 35 A. N. Zelikin, A. L. Becker, A. P. R. Johnston, K. L. Wark, F. Turatti and F. Caruso, *ACS Nano*, 2007, **1**, 63–69.
- 36 V. Kozlovskaya, E. Kharlampieva, I. Erel and S. A. Sukhishvili, *Soft Matter*, 2009, **5**, 4077–4087.
- 37 C. R. Kinnane, G. K. Such, G. Antequera-Garcia, Y. Yan, S. J. Dodds, L. M. Liz-Marzan and F. Caruso, *Biomacromolecules*, 2009, **10**, 2839–2846.
- 38 A. Diaspro, D. Silvano, S. Krol, O. Cavalleri and A. Gliozzi, *Langmuir*, 2002, **18**, 5047–5050.
- 39 S. Krol, M. Nolte, A. Diaspro, D. Mazza, R. Magrassi, A. Gliozzi and A. Fery, *Langmuir*, 2005, **21**, 705–709.
- 40 R. F. Fakhruллин, A. I. Zamaleeva, M. V. Morozov, D. I. Tazetdinova, F. K. Alimova, A. K. Hilmutdinov, R. I. Zhdanov, M. Kahraman and M. Culha, *Langmuir*, 2009, **25**, 4628–4634.
- 41 R. F. Fakhruллин, J. Garcia-Alonso and V. N. Paunov, *Soft Matter*, 2010, **6**, 391–397.
- 42 S. De Koker, B. G. De Geest, C. Cuvelier, L. Ferdinande, W. Deckers, W. E. Hennink, S. De Smedt and N. Mertens, *Adv. Funct. Mater.*, 2007, **17**, 3754–3763.
- 43 B. Staedler, R. Chandrawati, A. D. Price, S. F. Chong, K. Breheny, A. Postma, L. A. Connal, A. N. Zelikin and F. Caruso, *Angew. Chem., Int. Ed.*, 2009, **48**, 4359–4362.
- 44 T. Bieber, W. Meissner, S. Kostin, A. Niemann and H. P. Elsasser, *J. Controlled Release*, 2002, **82**, 441–454.
- 45 W. T. Godbey, K. K. Wu and A. G. Mikos, *J. Biomed. Mater. Res.*, 1999, **45**, 268–275.
- 46 M. Germain, P. Balaguer, J.-C. Nicolas, F. Lopez, J.-P. Esteve, G. B. Sukhorukov, M. Winterhalter, H. Richard-Foy and D. Fournier, *Biosens. Bioelectron.*, 2006, **21**, 1566–1573.
- 47 J. T. Wilson, W. Cui and E. L. Chaikof, *Nano Lett.*, 2008, **8**, 1940–1948.
- 48 J. T. Wilson, V. R. Krishnamurthy, W. Cui, Z. Qu and E. L. Chaikof, *J. Am. Chem. Soc.*, 2009, **131**, 18228–18229.

- 49 I. Erel-Unal and S. A. Sukhishvili, *Macromolecules*, 2008, **41**, 3962–3970.
- 50 D. M. Hushulian, V. A. Fechina, S. V. Kazakov, I. Y. Sakharov and I. G. Gazaryan, *Biochemistry*, 2003, **68**, 1006–1011.
- 51 J. Takebayashi, A. Tai and I. Yamamoto, *Biol. Pharm. Bull.*, 2003, **26**, 1368–1370.
- 52 T. G. Shutava, V. E. Agabekov and Y. M. Lvov, *Russ. J. Gen. Chem.*, 2007, **77**, 1494–1501.
- 53 A. Goffeau, B. G. Barrell, H. Bussey, R. W. Davis, B. Dujon, H. Feldmann, F. Galibert, J. D. Hoheisel, C. Jacq, M. Johnston, E. J. Louis, H. W. Mewes, Y. Murakami, P. Philippsen, K. Tettelin and S. G. Oliver, *Science*, 1996, **274**, 546.
- 54 S. A. Richman, D. M. Kranz and J. D. Stone, Biosensor Detection Systems: Engineering Stable, High Affinity Bioreceptors by Yeast Surface, in *Biosensors and Biodetection*, ed. A. Rasooly and K. E. Herold, Human Press, New Jersey, 2009, 504, ch. 19, pp. 323–350.
- 55 S. Shibasaki, M. Ueda, T. Iizuka, M. Hirayama, Y. Ikeda, N. Kamasawa, M. Osumi and A. Tanaka, *Appl. Microbiol. Biotechnol.*, 2001, **55**, 471–475.
- 56 R. Narayanaswamy, M. Levy, M. Tsechansky, G. M. Stovall, J. D. O'Connell, J. Mirrielees, A. D. Ellington and E. E. Marcotte, *Proc. Natl. Acad. Sci. U. S. A.*, 2009, **106**, 10147.
- 57 K. M. Slade, R. Baker, M. Chua, N. L. Thompson and G. Pielak, *Biochemistry*, 2009, **48**, 5083–5089.
- 58 I. Herskowitz, *Microbiol. Rev.*, 1988, **52**, 536–553.
- 59 T. G. Shutava, S. S. Balkundi, O. Vangala, J. J. Steffan, R. L. Bigelow, J. A. Cardelli, D. P. O'Neal and Y. M. Lvov, *ACS Nano*, 2009, **3**, 1877–1885.
- 60 K. M. Riedl and A. E. Hagerman, *J. Agric. Food Chem.*, 2001, **49**, 4917.
- 61 G. K. B. Lopes, H. M. Schulman and M. Hermes-Lima, *Biochim. Biophys. Acta*, 1999, **1472**, 142–152.
- 62 V. Kozlovskaya, E. Kharlampieva, I. Drachuk, D. Cheng and V. V. Tsukruk, *Soft Matter*, 2010, **6**, 3596–3608.
- 63 C. Brunot, L. Ponsonnet, C. Lagneau, P. Farge, C. Picart and B. Grosogeat, *Biomaterials*, 2007, **28**, 632–640.
- 64 B. J. Dutka, N. Nyholm and J. Petersen, *Water Res.*, 1983, **17**, 1363–1367.
- 65 U. J. Strotmann, B. Butz and W.-R. Bias, *Ecotoxicol. Environ. Saf.*, 1993, **25**, 79–88.
- 66 W. C. Mak, K. W. Sum, D. Traau and R. Renneberg, *IEE Proc.: Nanobiotechnol.*, 2004, **151**(2), 67–71.
- 67 T. Zhang, L. Ge and H. Chi, *Bull. Chem. Soc. Jpn.*, 2008, **81**, 906–911.
- 68 A. A. Antipov, G. B. Sukhorukov, E. Donath and H. Mohwald, *J. Phys. Chem. B*, 2001, **105**, 2281–2284.
- 69 R. von Klitzing and H. Mohwald, *Macromolecules*, 1996, **21**, 6901–6906.
- 70 E. Kharlampieva and S. A. Sukhishvili, *Polym. Rev.*, 2006, **46**, 377–395.
- 71 L. Payet, A. Ponton, L. Leger, H. Herve, J. L. Grossiord and F. Agnely, *Macromolecules*, 2008, **41**, 9376–9381.
- 72 C. Jiang, S. Markutsya and V. V. Tsukruk, *Adv. Mater.*, 2004, **16**, 157–166.
- 73 C. Jiang, S. Singamaneni, E. Merrick and V. V. Tsukruk, *Nano Lett.*, 2006, **6**, 2254–2259.
- 74 A. J. Nolte, M. F. Rubner and R. E. Cohen, *Macromolecules*, 2005, **38**, 5367–5370.
- 75 B.-S. Kim, H. Lee, Y. Min, Z. Poon and P. T. Hammond, *Chem. Commun.*, 2009, 4194–4196.
- 76 V. Kozlovskaya, A. Shamaev and S. A. Sukhishvili, *Soft Matter*, 2008, **4**, 1499–1507.
- 77 D. Pristiniski, V. Kozlovskaya and S. A. Sukhishvili, *J. Opt. Soc. Am. A*, 2006, **23**, 2639–2644.
- 78 V. V. Tsukruk and D. H. Reneker, *Polymer*, 1995, **36**, 1791–1808.
- 79 N. Elsner, F. Dubreuil and A. Fery, *Phys. Rev. E: Stat., Nonlinear, Soft Matter Phys.*, 2004, **69**, 031802.
- 80 M. E. McConney, S. Singamaneni and V. V. Tsukruk, *Polym. Rev.*, 2010, **50**, 235–286.
- 81 K. Glinel, G. B. Sukhorukov, H. Mohwald, V. Khrenov and K. Tauer, *Macromol. Chem. Phys.*, 2003, **204**, 1784–1790.
- 82 G. Ibarz, L. Dähne, E. Donath and H. Mohwald, *Chem. Mater.*, 2002, **14**, 4059–4062.
- 83 K. Glinel, M. Dubois, J.-M. Verbavatz, G. B. Sukhorukov and T. Zemb, *Langmuir*, 2004, **20**, 8546–8551.
- 84 A. A. Antipov, G. B. Sukhorukov, E. Donath and H. Mohwald, *J. Phys. Chem. B*, 2001, **105**, 2281–2284.